Hepatic clearance prediction of eight HIV protease inhibitors in rat

Tom De Bruyn, Patrick F. Augustijns and Pieter P. Annaert

Drug Delivery and Disposition, KU Leuven Department of Pharmaceutical and Pharmacological Sciences, O&N2, Herestraat 49 box 921, 3000 Leuven, Belgium (TDB, PFA, PPA).

Running title: Clearance of HIV protease inhibitors in rat

Corresponding Author:

Pieter Annaert, PhD

Drug Delivery and Disposition

KU Leuven Department of Pharmaceutical and Pharmacological Sciences

O&N2, Herestraat 49 – bus 921

B-3000 Leuven, Belgium.

Tel: 32-16-330303

Fax: 32-16-330305

E-mail: pieter.annaert@pharm.kuleuven.be

Abbreviations:

APV, amprenavir; ATZ, atazanavir; DRV, darunavir; FBS, fetal bovine serum; HEPES, 4-(2-hydroxyethyl)-1-piperazine ethanesulfonic acid; HIV, human immunodeficiency virus; IDV, indinavir; IVIVE, *in vitro – in vivo* extrapolation; LPV, lopinavir; NLV, nelfinavir; MPPGL, mg protein per gram liver; NTCP/Ntcp, sodium taurocholate cotransporting polypeptide; OATP/Oatp, Organic Anion Transporting Polypeptide (Human/Rat); PBS, phosphate buffered saline; PI, protease inhibitor; RTV, ritonavir; SLC, solute-linked carrier; SQV, saquinavir.

Abstract

This study aimed to determine the rate-limiting step in the overall hepatic clearance (CL_{hep}) of the marketed HIV protease inhibitors (PI) in rats by predicting the experimentally determined hepatic *in vivo* clearance of these drugs based on *in vitro* clearance values for uptake and/or metabolism. *In vitro* uptake and metabolic clearance values were determined in suspended rat hepatocytes and rat liver microsomes, respectively. *In vivo* CL_{hep} was determined after intravenous bolus administration in rats. Excellent *in vitro-in vivo* correlation (IVIVC, $R^2 = 0.80$) was observed when metabolic intrinsic Cl values were used, which were determined *in vitro* at a single concentration corresponding to the blood concentration observed in rats *in vivo* at the mean residence time. On the contrary, poor IVIVC was observed when *in vitro* metabolic Cl values based on full Michaelis-Menten profiles were used. In addition, the use of uptake Cl values or a combination of both uptake and metabolic clearance data led to poor predictions of *in vivo* clearance. Although our findings indicate a key role for metabolism in the CL_{hep} of several HIV PI in rats, subsequent simulations revealed that inhibition of hepatic uptake can lead to altered CL_{hep} for several of these drugs.

Introduction

Prediction of *in vivo* clearance values of drug candidates based on *in vitro* data (or *in vitro in vivo* extrapolation – IVIVE - for drug clearance) has become an essential activity during the preclinical phases of contemporary drug development programs. As reported in the companion paper by De Bruyn et al. (2015), clearance predictions with *in vitro* models derived from human liver tissue allow estimating a safe first-in-human dose to initiate clinical trials. *In vivo* drug clearance prediction in rats on the other hand, as applied in the present paper, is useful from different perspectives. First of all, accurate knowledge of the pharmacokinetic behavior of drug candidates in preclinical species (as compared to man) supports optimal design of toxicity studies with sensible use of animals. Secondly, as *in vivo* PK profiles can also be obtained in animals via various routes of administration (including the intravenous route) and under standardized conditions for a series of compounds (cfr. the present study), *in vitro in vivo* comparisons become highly relevant and may provide opportunities to fine tune IVIVE algorithms for drug clearance.

For compounds undergoing primarily hepatic elimination*, in vivo* clearance predictions are based on the extrapolation of *in vitro* data covering all hepatic drug elimination processes. These processes may include hepatic sinusoidal uptake, metabolism and/or biliary excretion, resulting in an entangled interplay which complicates the extrapolation to the *in vivo* situation.[1,2] Additionally, drug binding and sequestration equilibria will affect the overall impact of these processes.

Both microsomes and suspended hepatocytes have successfully been used for predicting the metabolic clearance of many compounds.[3–7] However, these model systems fail to

quantitatively predict the *in vivo* clearance of drugs for which active uptake transport forms the rate-limiting step in the overall hepatic clearance.[8] For these compounds, better *in vitro – in vivo* correlations are observed when *in vitro* uptake clearance values are measured and extrapolated to *in vivo* parameters.[9] Thus, with the recognition that transport proteins can significantly influence hepatic clearance (even for compounds that largely depend on metabolic enzymes for their clearance), typical pharmacokinetic models used for IVIVE of hepatic clearance had to be modified.[10] This has led to the development of IVIVE models implementing multiple hepatic disposition processes measured with various *in vitro* methods.[11,12] Consequently, such models can be used to gain information about the interplay between various hepatic elimination processes and the rate-limiting step in the overall hepatic clearance of drugs.

For the purpose of the present study on drug clearance prediction in rat, all marketed HIV protease inhibitors (PI) were included as model compounds. Since the predominant role of drug metabolizing enzymes in hepatobiliary disposition of HIV PI is generally considered as obvious, the potential role of transporters in disposition of these antiretroviral drugs has remained somewhat controversial. Nevertheless, interactions of HIV PI with transporters have been described. HIV PI are potent inhibitors of the sodium taurocholate-cotransporting polypeptide Ntcp [13] and several members of the organic anion transporting polypeptide family Oatp [14] in rat hepatocytes. In addition, HIV PI are substrates of several efflux transporters.[15,16] Extensive metabolism by cytochrome P450 enzymes has been explored in rat liver microsomes.[17,18] Thus, a complex interplay between multiple processes defines the hepatic disposition and clearance of HIV PI in rats. By directly comparing the rate of uptake into rat hepatocytes and the rate of

metabolism in rat hepatocytes and rat liver microsomes, Parker and Houston indicated that at low substrate concentrations hepatic uptake is the rate limiting step in the overall hepatic clearance of nelfinavir, saquinavir and ritonavir in rats.[19] In addition, they showed that this uptake process is extremely rapid and therefore suggested that the hepatic clearance of these three HIV PI is still blood flow limited in the *in vivo* situation.

The aim of this study was to accurately delineate the respective roles of enzymes and transporters in the overall hepatic elimination of all commercially available HIV PI in rats. Therefore, *in vitro* uptake data in suspended rat hepatocytes and metabolic data in rat liver microsomes were extrapolated to the hepatic *in vivo* clearance for all HIV PI and compared to experimentally determined *in vivo* blood clearance in rats. The same approach was applied for this series of compounds in man (see companion paper De Bruyn et al., 2015), providing unique data sets for detailed cross-species comparison of pharmacokinetic behaviour of these compounds. At the same time, possible species-specific aspects of clearance prediction algorithms (IVIVE) may be identified.

Materials and Methods

Chemicals. Ritonavir, indinavir sulfate, saquinavir mesylate, nelfinavir mesylate were obtained from Hetero Drugs Limited (Hyderabad, India). Atazanavir was provided by Bristol-Myers Squibb (New Brunswick, NJ) and amprenavir, darunavir, lopinavir and tipranavir were obtained through the NIH AIDS Reagent Program. William's E medium, Hanks' Balanced Salt Solution (HBSS), L-glutamine, Fetal Bovine Serum (FBS), penicillin-streptomycin mixture (contains 10,000 IU potassium penicillin and 10,000 µg streptomycin sulfate per ml in 0.85% saline) and Trypsin EDTA were purchased from Lonza SPRL (Verviers, Belgium). HEPES (4-(2- hydroxyethyl)-1-piperazine-ethanesulfonic acid) was purchased from MP Biochemical (Illkirch, France). Mineral oil was purchased from Acros organics (Thermo Scientific, Geel, Belgium). Collagenase (Type IV). Cyclosporin A, NADPH, Glucose-6-phosphate, $MgCl_2$ and silicon oil were obtained from Sigma-Aldrich (Schnelldorf, Germany).

Animals. All rats were housed according to the Belgian and European laws, guidelines and policies for animal experiments, housing and care in the central animal facilities of the university. The Institutional Ethical Committee for Animal Experimentation granted approval for this project.

Isolation of rat hepatocytes. Hepatocytes were isolated from male Wistar (170 – 200 g) rats using a 2-step collagenase perfusion, as described previously.[20] After isolation, cells were centrifuged (50 *g*) for 3 min at 4°C and the pellet was re-suspended in William's E medium supplemented with 5 % FBS, 2 mM L-glutamine, 100 IU/ml penicillin and 100 µg/ml streptomycin. Hepatocytes were counted using a hemocytometer and cell viability

(> 90 %) was determined using Trypan blue exclusion. Freshly-isolated rat hepatocytes were re-suspended in Krebs-Henseleit Buffer (NaCl 130 mM, KCl 5.17 mM, $CaCl_2$ 1.2 mM, $MgCl_2$ 1.2 mM, HEPES 12.5 mM, glucose 11.1 mM, Na-pyruvate 5 mM; pH 7.4) and kept on ice until start of the experiment.

Uptake experiments with suspended hepatocytes. All experiments with suspended hepatocytes were conducted as described previously.[14] Briefly, 500 µl of a double-concentrated cell suspension (2 million cells/ml) was pre-incubated for 10 min at 37°C. Subsequently, 500 µl of a double-concentrated substrate solution (2 µM) was added to initiate the incubation at 37°C (or 4°C to determine the non-saturable uptake component). After an incubation period of 30 sec, triplicate 200 µl aliquots of the suspension were immediately transferred to 1.5 ml ice-cold microcentrifuge tubes, containing 700 µl of an oil layer (silicone / mineral oil mixture; density, 1.015) above 300 µl of 8 % NaCl solution. Subsequently, the tubes were centrifuged for 2 min at 16,000 *g* using a tabletop centrifuge (Eppendorf 5415 C, Hamburg Germany). After freezing microcentrifuge tubes in dry ice, the conical tube ends were cut and the contents diluted in 300 µl of a 70/30 % methanol/water mixture. Samples were stored at -20 °C until analysis.

Preparation of rat liver microsomes (RLM). Briefly, three male Wistar rats (197-200 g) were fasted for 24 h prior to preparation of RLM. After rats were anesthetized with an intraperitoneal injection of 120 mg/kg of ketamine and 24 mg/kg xylazine, the livers were perfused with ice-cold oxygentated homogenization buffer (5 mM 3-(N-morpholino)-propanesulfonic acid MOPS, 1 mM EDTA, 250 mM sucrose, pH 7.4) to remove all blood. Subsequently, the livers were excised, minced with surgical scissors and added to ice-cold homogenization buffer (3 mL/g tissue). The tissue mixture was further

homogenized in a glass/Teflon© potter at 4°C. The pooled tissue solution was sampled for CYP content determination and centrifuged (4000 *g*) for 10 min at 4°C. After suspending the resulting pellet with homogenization buffer and repeating the centrifugation step, the supernatants were combined and transferred to polycarbonate ultracentrifuge tubes (Fisher Scientific, Landsmeer, Netherlands). This solution was subjected to another centrifugation step (15,000 *g*) for 20 min at 4°C, after which the pellet was discarded and the supernatant was ultra-centrifuged (150,000 g) for 70 min at 4°C. The resulting microsomal pellet was washed with homogenization buffer and ultracentrifugation was repeated (150,000 *g*) for 35 min at 4°C. The microsomal pellet was homogenized in microsomal storage buffer (5 mM MOPS, 1 mM EDTA, 20 % w/v glycerol) with a glass/Teflon© potter homogenizer (2-3 up- en downstrokes, 800 rpm). A sample of the microsomes was taken for protein content determination and aliquots (500 µL) were stored at -80°C.

Determination of metabolic clearance using rat liver microsomes. Incubations were performed in 48-well plates in a Thermomixer (Eppendorf AG, Hamburg, Germany) set at 37 °C and 350 rpm in a volume of 400 µL. Pooled rat liver microsomes were diluted in phosphate buffer (100 mM, pH 7.4) containing glucose-6-phosphate (3 mM) and $MgCl_2$ (3 mM). Parent depletion by rat liver microsomes (0.025 – 0.25 mg protein/ ml) was measured in triplicate incubations over a range of substrate concentrations (0.02 – 5 µM). After a pre-incubation period of 10 min, NADPH (1 mM) was added to initiate the reaction. To terminate the reaction, triplicate samples (75 µL) were quenched at 0, 10, 20 and 30 min by adding them to acetonitrile (75 µL) containing the internal standard. Samples were stored at -20 °C until analysis by mass spectrometry.

Determination of *in vivo* blood clearance of HIV PI in rats. The *in vivo* blood clearance $Cl_{in\ vivo,\ obs}$ of HIV PI was determined in male Wistar rats (350 – 420 g). HIV PI dissolved in 1:1:2 mixtures of ethanol:DMSO:saline were administered intravenously via the lateral tail vein at 10 mg/kg (except for SQV; 5 mg/kg). The administered volume was 1 ml/kg. Blood samples (200 µL) were collected from the opposite lateral tail vein at 5, 10, 20, 30, 60, 120, 180 and 240 min after dosing. Additionally, plasma samples were taken after 30, 60 and 120 min to determine the total blood-plasma drug concentration ratio C_b/C_p. Blood and plasma samples were stored at -20 °C until analysis.

Determination of unbound fraction in microsomal buffer. The unbound fraction in microsomal buffer was determined by equilibrium dialysis using HTD96b from HTDialysis, LLC (Gales Ferry, CT, US). The dialysis membranes were hydrated according to the manufacturer's instructions. The donor and acceptor compartment were filled with microsomal buffer containing the HIV protease inhibitor (10 µM) and PBS, respectively. Samples (n = 6) of both compartments were taken after 6 h and were stored at -20 °C until analysis.

Sample preparation and analysis. Samples obtained from liver microsomes and suspended rat hepatocytes were vortexed and centrifuged at 10,000 *g* for 10 min. Blood and plasma samples (30 µL) were diluted in 120 µL of water, followed by the addition of 300 µL of acetonitrile (containing the internal standard). Subsequently, samples were vortexed and centrifuged at 14,000 *g* for 10 min at room temperature. For all samples, the supernatant obtained after sample preparation was directly injected into the HPLC-tandem mass spectrometry system.

Analysis of HIV protease inhibitor was performed with a Thermo Scientific (San Jose, USA) LC–MS/MS system comprising an Accela® autosampler, an Accela® pump and a TSQ Quantum Access® triple quadrupole mass spectrometer equipped with an electrospray ionization (ESI) source. A Kinetex® XB - C18 column (50 mm × 2.1 mm, 2.6 μm), protected by a SecurityGuard ULTRA precolumn (Phenomenex, The Netherlands) was used for all chromatographic separations. The mobile phase consisted of a 0.5 mM ammonium acetate buffer (pH 3.5) (A) and methanol (B). Gradient elution at a constant flow rate of 400 μL/min was performed as follows: 95 % A decreased linearly to 5 % A in 2 min; constant flow of 5 % A for 1 min; linear increase back to 95 % A in 10 sec; re-equilibration for 1.0 min with 95 % A before the next injection. The total run time was 4.0 min and the injection volume was 10 μL (partial loop mode). The column oven and the autosampler tray temperature were set at 30° and 15 °C, respectively. The mass spectrometer was operated in the positive electrospray mode. The spray voltage was 3000 V and argon was used as the collision gas at a pressure of 1.5 mTorr. The mass spectrometer was operated in a 3-channel selected reaction monitoring (SRM) mode with a scan time of 100 ms. Transitions monitored, automatically optimized parameters and retention times are listed in Supplemental Table 1. Data acquisition and peak integration were performed with Xcalibur software Thermo Scientific (San Jose, USA).

Data Analysis.

Uptake clearance data. Net uptake values were obtained by subtracting uptake in rat hepatocytes at 4°C from total uptake at 37°C. Subsequently, active, passive and total uptake clearance values (μL/min/million cells) were calculated by dividing the net uptake,

passive uptake or total uptake (pmol/min/million cells) by the corresponding substrate concentration, respectively.

Metabolic clearance data. For metabolic drug depletion experiments, the log of the drug concentration was plotted in function of time and the elimination constant was calculated by fitting a single exponential decay. This elimination constant was used to calculate the half-life of the metabolic turn-over, which was further converted to the apparent intrinsic metabolic clearance (µl/min/mg protein) $Cl_{app\ int,\ met}$ according to following equation:[21]

$$Cl_{app\ int,met} = \frac{0.693}{t_{1/2}} \times \frac{incubation\ volume}{mg\ protein} \quad (1)$$

Intrinsic metabolic clearance values were corrected for the unbound fraction fu_{mic} to obtain the intrinsic metabolic clearance $Cl_{int,met}$.

In vivo pharmacokinetic data. In vivo pharmacokinetic parameters were calculated using non-compartmental analysis. Both AUC (area under the curve of the blood concentration – time plot) and AUMC (area under the curve when plotting the blood concentration x time versus time) were calculated using the trapezoidal rule and extrapolated to infinity with the terminal elimination rate constant λ. *In vivo* blood clearance (regarded as the hepatic clearance by assuming that the urinary excretion of HIV PI is negligible) and distribution volume were calculated according to following equations:

$$\mathrm{Cl_B} = \frac{\mathrm{Dose}}{\mathrm{AUC}} \quad (2) \qquad Vd = \frac{\mathrm{Cl_B}}{\mathrm{k}} \quad (3)$$

The mean residence time (MRT) was calculated according to following equation:

$$\mathrm{MRT} = \frac{\mathrm{AUMC}}{\mathrm{AUC}} \quad (4)$$

In vitro – in vivo extrapolations. To evaluate the rate-limiting step in the overall hepatic elimination of HIV PI, the experimentally determined *in vivo* clearance of HIV PI was

predicted based on uptake data only, metabolism data only or a combination of both. Therefore, the determined *in vitro* intrinsic uptake or metabolic clearance values were first scaled to the intrinsic *in vivo* clearance by following reported scaling factors; values used for hepatocellularity and MPPGL were 120 × 10^6 cells/g liver and 46 mg protein/g liver, respectively.[22,23] The rat liver weight/kg body weight was determined in house and amounted to 40 g liver/kg. According to the well-stirred model, the intrinsic *in vivo* clearance values were converted to *in vivo* blood Clearance (Cl_B) values according to following equations;[11,24]

$$Cl_B = \frac{Q_B \times fu'_B \times Cl_{int,met}}{Q_B + fu'_B \times Cl_{int,met}} \quad (5)$$

$$Cl_B = \frac{Q_B \times fu'_B \times Cl_{int,upt\ total}}{Q_B + fu'_B \times Cl_{int,upt\ total}} \quad (6)$$

$$Cl_B = \frac{Q_B \times fu'_B \times Cl_{int,upt\ total} \times Cl_{int,met}}{Q_B \times (Cl_{int,met} + Cl_{int,upt\ passive}) + (fu'_B \times Cl_{int,upt\ total} \times Cl_{int,met})} \quad (7)$$

With Q_B, the blood flow in rats (55.2 ml/min/kg), Hc the hematocrit (0.56) and fu'$_B$ the fraction unbound in blood, calculated according to following equation;

$$fu'_B = fu \times (1 - Hc) \times (\frac{1}{Rb}) \quad (8)$$

With fu, the free fraction in plasma and Rb the blood to plasma partitioning coefficient.

Interaction simulations. To simulate the impact of interaction with active hepatic uptake of HIV PI, active uptake clearance was arbitrarily set at 10 or 500 % of the experimentally determined control value. Subsequently, the impact of inhibition and induction of active uptake transport on overall hepatic clearance was calculated by calculating the

corresponding *in vivo* hepatic clearance according to equation 7. Hepatic clearance values under the simulated conditions were expressed as a percentage of the calculated clearance values under control conditions.

Statistics. The data analysis tool in Microsoft Excel 2010 (*t*-test, $p < 0.05$) was used to evaluate statistical differences between uptake under control condition and the presence of inhibitors.

Results

Uptake of HIV PI in suspended rat hepatocytes.

The passive and active uptake clearance values of all HIV PI in suspended rat hepatocytes are summarized in Table 1. For all HIV PI, the total uptake clearance at 37 °C was significantly reduced when experiments were conducted at 4 °C. The relative contribution of the passive uptake in the total uptake of HIV PI ranged from 8 % for indinavir and atazanavir to 58 % for nelfinavir. Passive uptake clearance was positively correlated ($R^2 = 0.7$) with LogP, as illustrated in Supplemental Figure 1.

To further illustrate the involvement of carrier-mediated transport in the hepatic uptake of HIV PI, the effect of the non-specific inhibitor cyclosporin A (5 μM) on the hepatic uptake of indinavir and atazanavir was studied (Supplemental Figure 2). Cyclosporin is known to inhibit both uptake and efflux transporters as well as metabolizing enzymes.[25–28] However, under the experimental conditions used in this study (e.g. experiments in suspended hepatocytes at short time points), minimal impact of CYP-mediated metabolism or involvement of efflux transporters is assumed. In addition, the possible effects of cyclosporin A on metabolism or efflux would have implied increased substrate uptake. Instead, cyclosporin A significantly decreased the uptake of indinavir and atazanavir under control conditions by 44 % and 46 %, respectively.

Metabolic clearance of HIV PI in rat liver microsomes.

The intrinsic metabolic clearance $Cl_{int,\ met}$ of HIV PI was determined in pooled rat liver microsomes (Supplemental Figure 3). Metabolic parameters describing Michaelis-Menten type kinetics were obtained for seven HIV PI and are summarized in Table 2. The intrinsic metabolic clearance values for ritonavir and nelfinavir were taken from published data by Parker and Houston.[19] Additionally, metabolic clearance was measured

at one concentration corresponding to the *in vivo* unbound blood concentration after a time window corresponding to the mean residence time (Table 3).

***In vivo* pharmacokinetics of HIV PI in rats after intravenous administration.**

All HIV PI were formulated in a mixture of ethanol, DMSO and saline (ratio 1:1:2). To test the potential impact of DMSO on the *in vivo* clearance of HIV PI, the *in vivo* pharmacokinetics of indinavir dissolved in a mixture of ethanol, dextrose and water (ratio 3:3:4) was also measured. There was no significant difference in *in vivo* blood clearance values or other pharmacokinetic parameters between both formulations (data not shown).

All HIV PI were cleared rapidly in rats following intravenous administration. Blood concentration – time profiles are shown for all HIV PI in Supplemental Figure 4 and corresponding *in vivo* pharmacokinetic parameters are summarized in Table 4. *In vivo* blood clearance values ranged from 2.2 ± 0.4 ml/min/kg for tipranavir to 47.0 ± 1.1 ml/min/kg for lopinavir.

IVIVE of the hepatic clearance of HIV PI in rats

The *in vitro* intrinsic clearance values for uptake ($Cl_{upt,\ active}$ and $Cl_{upt,\ passive}$) and metabolism ($Cl_{int,met}$) were scaled to the whole liver by applying corresponding scaling factors (Table 5). Plasma protein binding and blood-to-plasma ratios were experimentally determined and are summarized in Table 6. Subsequently, these *in vitro* clearance values were extrapolated to the *in vivo* blood clearance based on the individual processes or the combination of both according to equations 5, 6 and 7, respectively.

The relationship between the experimentally determined and predicted *in vivo* blood clearance of all HIV PI is shown in Figure 1. Based on uptake data only (Figure 1, panel A), a poor linear correlation (R^2 = 0.25) between the reported and predicted *in vivo*

clearance was found. However, only for ritonavir the predicted *in vivo* blood clearance deviated by more than 2 fold from the experimentally determined value. Especially for indinavir, atazanavir, nelfinavir and saquinavir, extrapolated uptake clearance values in hepatocytes predicted the observed *in vivo* blood clearance well (max 1.2 fold difference).

When IVIVE was based on full pharmacokinetic metabolism data (Figure 1, panel B), *in vivo* blood clearance values were over-estimated for all HIV PI. Moreover, all predicted *in vivo* blood clearance values (except for tipranavir) seemed to approach the hepatic blood flow. On the contrary, when IVIVE was based on intrinsic metabolic clearance values ($Cl_{int,\ met}$) determined in rat liver microsomes at one relevant concentration (= the unbound concentration at the mean residence time calculated from the *in vivo* profiles), a good correlation ($R^2 = 0.80$) between the observed and predicted *in vivo* clearance values was observed (Figure 1, panel C). Except for ritonavir and tipranavir, clearance value estimates fell within a 1.5-fold range of the experimentally determined values.

When both uptake and metabolism processes were taken into account (Figure 1, panel D), the correlation between reported and predicted *in vivo* hepatic clearance was comparable to that based on uptake data only ($R^2 = 0.25$), with a fold deviation from the observed value ranging from 0.7 fold for tipranavir to 2 fold for ritonavir.

To simulate the impact of interaction with active hepatic uptake on the hepatic clearance of HIV PI, the effect of inhibition and induction of the hepatic uptake was calculated and presented in Figure 2. The simulation showed that the hepatic Cl of atazanavir, indinavir, lopinavir and tipranavir decreased approximately by 60 % when active hepatic uptake is inhibited by 90 %. On the contrary, a limited decrease of the hepatic Cl for other HIV PI

is observed when active uptake was inhibited. The predicted effect of induction of transporter expression on the hepatic Cl of hepatocytes revealed a significant increase in the hepatic Cl of tipranavir when hepatic uptake was 5 times increased, whereas only a limited effect was observed for other HIV PI. To evaluate potential species differences on the impact of active uptake inhibition, the relative contribution of hepatic uptake transport in the overall clearance for each individual HIV protease inhibitor was compared in rat and human ($R^2 = 0.74$; Figure 3). The simulated effect of hepatic uptake inhibition (90 %) on the overall hepatic clearance of HIV PI showed great agreement in rat and human. Indeed, in both species the hepatic clearance values of lopinavir, atazanavir and tipranavir are predicted to be influenced by hepatic uptake inhibition. On the contrary, amprenavir and nelfinavir will most likely not be influenced by basolateral uptake transporter mediated drug – drug interactions as victim drugs.

Discussion

Hepatic disposition of HIV protease inhibitors comprises of a complex network of multiple processes including transporter-mediated uptake/elimination and CYP-mediated metabolism.[15,16,29] Consequently, interference with any of these processes may result in clinically relevant drug – drug interactions. The present study aimed to elucidate the rate-limiting step in the overall hepatic clearance in rats and to evaluate the impact of hepatic uptake transport inhibition and induction for all marketed HIV PI.

Both rat hepatocytes in suspension and sandwich-culture configuration represent useful *in vitro* model systems for the assessment of hepatic uptake.[30–33] However, several publications have demonstrated that sandwich-cultured rat hepatocytes exhibit declining transport activity levels of most hepatic uptake transporters (belonging to the SLC gene family) in function of culture time.[34] Therefore, hepatocytes in suspension were used in this study to investigate transporter-mediated uptake clearance of HIV PI.[34] Uptake clearance values of all HIV PI, determined in suspended rat hepatocytes, were temperature-dependent (Table 1), suggesting the involvement of a carrier-mediated process in the hepatic uptake of HIV PI. Although the passive contribution may be partly influenced by alterations in membrane fluidity at 4 °C, the involvement of hepatic uptake transport proteins was further confirmed by the reduced hepatic uptake of indinavir and atazanavir in presence of the non-specific transporter inhibitor cyclosporin A (Supplemental Figure 2).[35] Parameters describing Michaelis-Menten kinetics would have been preferred to calculate intrinsic uptake clearance values of HIV PI. However, initial uptake velocities showed no saturation over the concentration range tested for several PI (e.g. indinavir) (data not shown). Therefore, we determined the uptake clearance of all

HIV PI at 1 μM (Table 1), a concentration well below the previously reported K_m values for nelfinavir, saquinavir and ritonavir.[19] Literature data regarding hepatic uptake of HIV PI in rat hepatocytes is scarce. Yabe et al. observed active uptake clearance values of 873 ± 216 and 293 ± 153 μl/min/million cells in suspended rat hepatocytes for ritonavir and saquinavir, respectively.[36] These data are comparable to our results and uptake clearance values reported by Parker and Houston.[19] The latter study additionally reported a net uptake clearance for nelfinavir (2670 μl/min/million cells), which is approximately 13-fold higher compared to our data.[19] This discrepancy may result from differences in experimental design (one concentration versus full kinetic profiles) and methodology (presence of albumin in the incubation medium).

Rat liver microsomes have shown to be a robust *in vitro* model system for the assessment of oxidative metabolism by CYP enzymes and for the prediction of hepatic metabolic clearance of large compound sets.[7,37] In addition to liver microsomes, phase I drug metabolism can be determined in suspended hepatocytes, which offer the additional advantage that phase II conjugation reactions (e.g. glucuronidation) can also be studied.[38] However, it is well known that uptake transporters present in hepatocytes can increase metabolic clearance by elevating the concentration at the site of the metabolizing enzymes.[12] Assuming that phase II conjugation pathways are not significantly influencing the overall elimination of HIV PI, a pooled batch of rat liver microsomes was used to study transporter-independent oxidative metabolism. Parameters describing Michaelis-Menten type kinetics were obtained for seven HIV PI (Table 2). Due to low apparent K_m values, analytical sensitivity limited accurate determination of the metabolic turnover rate at very low substrate concentrations for ritonavir and nelfinavir. Therefore, intrinsic

metabolic clearance values for these drugs were taken from literature.[19] In this publication, the metabolic clearance value for saquinavir was comparable to the value obtained in the present study.

Extrapolating *in vitro* metabolism data to gain quantitative predictions of the *in vivo* hepatic clearance has successfully been applied for compounds for which elimination is predominantly mediated by metabolic enzymes.[7,39,40] Consistently, *in vitro* transport data have been used to accurately predict the *in vivo* clearance of drugs, for which hepatic uptake is the rate-limiting step in the overall hepatic clearance.[9] However, the *in vivo* elimination of most drugs is defined by a complex interplay between transporters and metabolizing enzymes. Therefore, single parameter models have been expanded to more complex models, combining multiple processes of hepatic elimination.[10,11,41–43] In the present study, we retrospectively predicted experimentally determined *in vivo* blood clearance with single process models (based on *in vitro* metabolism or uptake data) as well as with a model combining both processes to further elucidate the rate-limiting step in the overall hepatic elimination of HIV PI.[12] Overall, IVIVE based on uptake data only resulted in a poor correlation ($R^2 = 0.25$) between predicted and observed *in vivo* blood clearance values (Figure 1, panel A). The significant overestimation of the *in vivo* blood clearance for darunavir, amprenavir and ritonavir is consistent with the observation that IVIVE based on uptake clearance data derived from hepatocytes results in an overestimation of hepatic clearance.[11] On the contrary, for other HIV PI (e.g. indinavir, nelfinavir, saquinavir and atazanavir) IVIVE resulted in a good quantitative prediction of the *in vivo* blood clearance values, suggesting that for these compounds hepatic uptake may be a more dominant process in the overall hepatic elimination in rats.

IVIVE using full Michaelis Menten profiles for metabolism in rat liver microsomes resulted in a poor correlation between predicted and observed *in vivo* blood clearance (R^2 = 0.47, Figure 1, Panel B). Interestingly, when single parameter IVIVE analysis was based on metabolism data performed at one concentration corresponding to the relevant *in vivo* concentration (= the unbound blood concentration at the mean residence time determined in the *in vivo* part of the present study) a good correlation (R^2 = 0.80) was observed (Figure 1, Panel C). This suggests that at relevant *in vivo* conditions, high intracellular unbound concentrations are reached at which metabolizing enzymes appear to be (partially) saturated. Consequently, the use of metabolism data based on full *in vitro* concentration profiles in rat liver microsomes results in an overestimation of the hepatic *in vivo* clearance. Indeed, as already indicated previously by Parker and Houston, microsomal clearance values (determined as V_{max} / K_m) can be misleading in terms of the magnitude of the metabolic turnover *in vivo.*[19] Compared to the approaches based on hepatic metabolism or uptake only, IVIVE based on both metabolism and transporter data showed a poor correlation between predicted and observed *in vivo* clearance values.

Inhibition of hepatic uptake is widely accepted as a mechanism explaining important drug-drug interactions in humans. More recently, induction of hepatic uptake transporters has also been suggested to explain the effect of rifampicin on the pharmacokinetics of digoxin and glyburide.[44,45] To assess the impact of hepatic uptake transport inhibition or induction, the sensitivity of overall Cl predictions towards alterations in active hepatic uptake Cl was evaluated for each individual HIV protease inhibitor (Figure 2). Because the extent of inhibition/induction of hepatic uptake in vivo is unknown, we anticipated a worst case scenario and evaluated conditions of 90 % inhibition or 5-fold induction. Our

data suggest that most HIV PI can be involved as victim drugs in drug – drug interactions in rats when active uptake is inhibited. Only for darunavir, amprenavir and nelfinavir, potent hepatic uptake inhibition is expected to marginally influence the hepatic Cl. Our simulations also showed that induction of hepatic uptake transporters may lead to an increased hepatic Cl of tipranavir. Interestingly, no effect of induction is predicted for other HIV PI, suggesting that the hepatic clearance of these HIV PI (e.g. indinavir, lopinavir and atazanavir) is blood-flow limited.

Finally, when we compared the relative contribution of hepatic uptake transport in the overall clearance for each individual HIV protease inhibitor in rat and human (see companion paper De Bruyn et al., 2015), a good correlation (R^2 = 0.74) between both species was observed (Figure 3). Indeed, when we simulated the effect of hepatic uptake inhibition on the overall clearance of HIV PI in rat and human, we noticed that in both species the hepatic clearance values of lopinavir, atazanavir and tipranavir are predicted to be influenced by hepatic uptake inhibition. On the contrary, amprenavir and nelfinavir are not expected to be influenced by uptake transporter mediated drug – drug interactions as victim drugs. The results for lopinavir are in good agreement with the increased plasma concentrations of lopinavir in presence of the 521 T>C gene polymorphism in SLCO1B1.[29]

In conclusion, these results confirm a key role for metabolism in the hepatic clearance of most HIV PI in rats. In addition, hepatic uptake transport may be important for several HIV PI, suggesting a complex transporter-metabolism interplay for these compounds. Our findings also imply that transporter-mediated drug-drug interactions at the level of rat liver involving several of these HIV PI as victim drugs cannot be excluded.

ACKNOWLEDGEMENTS

Tom De Bruyn received a PhD scholarship from the Agency for Innovation by Science and Technology, Flanders. This study was supported by grants from 'Fonds voor Wetenschappelijk Onderzoek', Flanders and 'Onderzoeksfonds' of the KU Leuven, Belgium.

References

1. Benet LZ. 2009. The drug transporter-metabolism alliance: uncovering and defining the interplay. Mol. Pharm. 6:1631–1643.

2. Lam JL, Benet LZ. 2004. Hepatic microsome studies are insufficient to characterize in vivo hepatic metabolic clearance and metabolic drug-drug interactions: studies of digoxin metabolism in primary rat hepatocytes versus microsomes. Drug Metab. Dispos. 32:1311–1316.

3. Houston JB, Carlile DJ. 1997. Prediction of hepatic clearance from microsomes, hepatocytes, and liver slices. Drug Metab. Rev. 29:891–922.

4. Naritomi Y, Terashita S, Kimura S, Suzuki A, Kagayama A, Sugiyama Y. 2001. Prediction of human hepatic clearance from in vivo animal experiments and in vitro metabolic studies with liver microsomes from animals and humans. Drug Metab. Dispos. 29:1316–1324.

5. Naritomi Y, Terashita S, Kagayama A, Sugiyama Y. 2003. Utility of hepatocytes in predicting drug metabolism: comparison of hepatic intrinsic clearance in rats and humans in vivo and in vitro. Drug Metab. Dispos. 31:580–588.

6. Obach RS, Baxter JG, Liston TE, Silber BM, Jones BC, MacIntyre F, Rance DJ, Wastall P. 1997. The prediction of human pharmacokinetic parameters from preclinical and in vitro metabolism data. J. Pharmacol. Exp. Ther. 283:46–58.

7. Riley RJ, McGinnity DF, Austin RP. 2005. A unified model for predicting human hepatic, metabolic clearance from in vitro intrinsic clearance data in hepatocytes and microsomes. Drug Metab. Dispos 33:1304–1311.

8. Soars MG, Grime K, Sproston JL, Webborn PJH, Riley RJ. 2007. Use of hepatocytes to assess the contribution of hepatic uptake to clearance in vivo. Drug Metab. Dispos. 35:859–865.

9. Watanabe T, Kusuhara H, Maeda K, Kanamaru H, Saito Y, Hu Z, Sugiyama Y. 2010. Investigation of the rate-determining process in the hepatic elimination of HMG-CoA reductase inhibitors in rats and humans. Drug Metab. Dispos. 38:215–222.

10. Soars MG, Webborn PJH, Riley RJ. 2009. Impact of hepatic uptake transporters on pharmacokinetics and drug-drug interactions: use of assays and models for decision making in the pharmaceutical industry. Mol. Pharm. 6:1662–1677.

11. Umehara K, Camenisch G. 2012. Novel in vitro-in vivo extrapolation (IVIVE) method to predict hepatic organ clearance in rat. Pharm. Res. 29:603–617.

12. Webborn PJH, Parker AJ, Denton RL, Riley RJ. 2007. In vitro-in vivo extrapolation of hepatic clearance involving active uptake: theoretical and experimental aspects. Xenobiotica 37:1090–1109.

13. McRae MP, Lowe CM, Tian X, Bourdet DL, Ho RH, Leake BF, Kim RB, Brouwer KLR, Kashuba ADM. 2006. Ritonavir, saquinavir, and efavirenz, but not nevirapine, inhibit bile acid transport in human and rat hepatocytes. J. Pharmacol. Exp. Ther. 318:1068–1075.

14. De Bruyn T, Ye Z-W, Peeters A, Sahi J, Baes M, Augustijns PF, Annaert PP. 2011. Determination of OATP-, NTCP- and OCT-mediated substrate uptake activities in individual and pooled batches of cryopreserved human hepatocytes. Eur J Pharm Sci 43:297–307.

15. Kis O, Robillard K, Chan GNY, Bendayan R. 2010. The complexities of antiretroviral drug-drug interactions: role of ABC and SLC transporters. Trends in Pharmacological Sciences 31:22–35.

16. Griffin L, Annaert P, Brouwer KLR. 2011. Influence of drug transport proteins on the pharmacokinetics and drug interactions of HIV protease inhibitors. J Pharm Sci 100:3636–3654.

17. Shibata N, Gao W, Okamoto H, Kishida T, Yoshikawa Y, Takada K. 2002. In-vitro and in-vivo pharmacokinetic interactions of amprenavir, an HIV protease inhibitor, with other current HIV protease inhibitors in rats. J. Pharm. Pharmacol. 54:221–229.

18. Yamaji H, Matsumura Y, Yoshikawa Y, Takada K. 1999. Pharmacokinetic interactions between HIV-protease inhibitors in rats. Biopharm Drug Dispos 20:241–247.

19. Parker AJ, Houston JB. 2008. Rate-limiting steps in hepatic drug clearance: comparison of hepatocellular uptake and metabolism with microsomal metabolism of saquinavir, nelfinavir, and ritonavir. Drug Metab. Dispos 36:1375–1384.

20. Annaert PP, Turncliff RZ, Booth CL, Thakker DR, Brouwer KLR. 2001. P-Glycoprotein-Mediated In Vitro Biliary Excretion in Sandwich-Cultured Rat Hepatocytes. Drug Metabolism and Disposition 29:1277 –1283.

21. Obach RS. 1999. Prediction of human clearance of twenty-nine drugs from hepatic microsomal intrinsic clearance data: An examination of in vitro half-life approach and nonspecific binding to microsomes. Drug Metab. Dispos. 27:1350–1359.

22. Bayliss MK, Bell JA, Jenner WN, Park GR, Wilson K. 1999. Utility of hepatocytes to model species differences in the metabolism of loxtidine and to predict pharmacokinetic parameters in rat, dog and man. Xenobiotica 29:253–268.

23. Davies B, Morris T. 1993. Physiological parameters in laboratory animals and humans. Pharm. Res. 10:1093–1095.

24. Yang J, Jamei M, Yeo KR, Rostami-Hodjegan A, Tucker GT. 2007. Misuse of the well-stirred model of hepatic drug clearance. Drug Metab. Dispos. 35:501–502.

25. Neuvonen PJ, Niemi M, Backman JT. 2006. Drug interactions with lipid-lowering drugs: mechanisms and clinical relevance. Clin. Pharmacol. Ther. 80:565–581.

26. Mita S, Suzuki H, Akita H, Hayashi H, Onuki R, Hofmann AF, Sugiyama Y. 2006. Inhibition of bile acid transport across Na+/taurocholate cotransporting polypeptide (SLC10A1) and bile salt export pump (ABCB 11)-coexpressing LLC-PK1 cells by cholestasis-inducing drugs. Drug Metab. Dispos. 34:1575–1581.

27. De Bruyn T, Van Westen GJP, Ijzerman AP, Stieger B, de Witte P, Augustijns PF, Annaert PP. 2013. Structure-based Identification of OATP1B1/3 Inhibitors. Mol. Pharmacol. 83:1257–67.

28. Zhou S-F. 2008. Structure, function and regulation of P-glycoprotein and its clinical relevance in drug disposition. Xenobiotica 38:802–832.

29. Hartkoorn RC, Kwan WS, Shallcross V, Chaikan A, Liptrott N, Egan D, Sora ES, James CE, Gibbons S, Bray PG, Back DJ, Khoo SH, Owen A. 2010. HIV protease inhibitors are substrates for OATP1A2, OATP1B1 and OATP1B3 and lopinavir plasma concentrations are influenced by SLCO1B1 polymorphisms. Pharmacogenet. Genomics 20:112–120.

30. Barton HA, Lai Y, Goosen TC, Jones HM, El-Kattan AF, Gosset JR, Lin J, Varma MV. 2013. Model-based approaches to predict drug-drug interactions associated with hepatic uptake transporters: preclinical, clinical and beyond. Expert Opin Drug Metab Toxicol 9:459–472.

31. Ramboer E, Vanhaecke T, Rogiers V, Vinken M. 2013. Primary hepatocyte cultures as prominent in vitro tools to study hepatic drug transporters. Drug Metab. Rev. 45:196–217.

32. Swift B, Pfeifer ND, Brouwer KLR. 2010. Sandwich-cultured hepatocytes: an in vitro model to evaluate hepatobiliary transporter-based drug interactions and hepatotoxicity. Drug Metab. Rev. 42:446–471.

33. Ye Z-W, Augustijns P, Annaert P. 2008. Cellular accumulation of cholyl-glycylamido-fluorescein in sandwich-cultured rat hepatocytes: kinetic characterization, transport mechanisms, and effect of human immunodeficiency virus protease inhibitors. Drug Metab. Dispos 36:1315–1321.

34. De Bruyn T, Chatterjee S, Fattah S, Keemink J, Nicolaï J, Augustijns P, Annaert P. 2013. Sandwich-cultured hepatocytes: utility for in vitro exploration of hepatobiliary drug disposition and drug-induced hepatotoxicity. Expert Opin Drug Metab Toxicol 9:589–616.

35. Poirier A, Lavé T, Portmann R, Brun M-E, Senner F, Kansy M, Grimm H-P, Funk C. 2008. Design, Data Analysis, and Simulation of in Vitro Drug Transport Kinetic Experiments Using a Mechanistic in Vitro Model. Drug Metabolism and Disposition 36:2434 –2444.

36. Yabe Y, Galetin A, Houston JB. 2011. Kinetic characterization of rat hepatic uptake of 16 actively transported drugs. Drug Metab. Dispos. 39:1808–1814.

37. Grime K, Riley RJ. 2006. The impact of in vitro binding on in vitro-in vivo extrapolations, projections of metabolic clearance and clinical drug-drug interactions. Curr. Drug Metab. 7:251–264.

38. Mano Y, Usui T, Kamimura H. 2007. Comparison of inhibition potentials of drugs against zidovudine glucuronidation in rat hepatocytes and liver microsomes. Drug Metab. Dispos. 35:602–606.

39. Ito K, Houston JB. 2004. Comparison of the use of liver models for predicting drug clearance using in vitro kinetic data from hepatic microsomes and isolated hepatocytes. Pharm. Res. 21:785–792.

40. McGinnity DF, Soars MG, Urbanowicz RA, Riley RJ. 2004. Evaluation of fresh and cryopreserved hepatocytes as in vitro drug metabolism tools for the prediction of metabolic clearance. Drug Metab. Dispos 32:1247–1253.

41. Camenisch G, Umehara K. 2012. Predicting human hepatic clearance from in vitro drug metabolism and transport data: a scientific and pharmaceutical perspective for assessing drug-drug interactions. Biopharm Drug Dispos 33:179–194.

42. Kusuhara H, Sugiyama Y. 2009. In vitro-in vivo extrapolation of transporter-mediated clearance in the liver and kidney. Drug Metab. Pharmacokinet. 24:37–52.

43. Shitara Y, Sato H, Sugiyama Y. 2005. Evaluation of drug-drug interaction in the hepatobiliary and renal transport of drugs. Annu. Rev. Pharmacol. Toxicol. 45:689–723.

44. Zheng H, Huang Y, Frassetto L, Benet L. 2009. Elucidating Rifampin's Inducing and Inhibiting Effects on Glyburide Pharmacokinetics and Blood Glucose in Healthy Volunteers: Unmasking the Differential Effect of Enzyme Induction and Transporter Inhibition for a Drug and Its Primary Metabolite. Clin Pharmacol Ther 85:78–85.

45. Lam JL, Shugarts SB, Okochi H, Benet LZ. 2006. Elucidating the effect of final-day dosing of rifampin in induction studies on hepatic drug disposition and metabolism. J. Pharmacol. Exp. Ther. 319:864–870.

FIGURE LEGENDS

Supplemental Figure 1

Relationship between LogP and passive uptake clearance for all HIV protease inhibitors in suspended rat hepatocytes. Passive uptake clearance values were experimentally determined at 4 °C and logP values were obtained from ChemSpider.

Supplemental Figure 2

Uptake of indinavir and atazanavir in suspended rat hepatocytes. Bars represent the uptake (1μM, 30 sec) determined at 37 °C (black bars), at 4 °C (open bars) or at 37 °C in the presence of cyclosporin A (5 μM, grey bars). * Statistically significant difference compared with control uptake determined at 37°C ($p < 0.05$).

Supplemental Figure 3

Relationship between metabolic rate and substrate concentration for all tested HIV PI in pooled rat liver microsomes. Points represent mean values (± SD) of triplicate incubations and the solid line represents the best fit to experimental data according to the Michaelis-Menten equation.

Supplemental Figure 4

Blood concentration – time profile of HIV PI following intravenous administration (10 mg/kg, except for saquinavir; 5 mg/kg) to male Wistar rats. Points represent mean values (± SD) of triplicate incubations and the solid line represents the best fit to experimental data according to a one-compartmental model.

Figure 1

Relationship between the experimentally determined and calculated *in vivo* clearance of all HIV PI in rats. Clearance values (ml/min/kg) were predicted based on only *in vitro*

uptake clearance data (A), only concentration-velocity profile-based *in vitro* metabolism data (B), only *in vitro* metabolic clearance data determined at one clinically relevant concentration (C) or a combination of both uptake and metabolic clearance data (D).

Figure 2

Simulation of the impact of interaction with hepatic uptake on the hepatic clearance of HIV PI. Hepatic clearance values of HIV PI are shown under conditions of 90 % inhibition (and/or down-regulation) (open bars) or 5-fold induction (and/or activation) (grey bars) of the hepatic uptake Cl and are expressed as a percentage of the calculated in vivo clearance under control conditions.

Figure 3

Correlation between rat and human regarding the simulated effect of hepatic uptake inhibition (90 %) on the overall hepatic clearance of HIV PI. Values represent predictions of residual hepatic clearance under conditions of 90 % inhibition of hepatic uptake Cl for each HIV PI in both species, and are expressed relative to the determined *in vivo* clearance for rat and human, respectively.

Supplemental Table 1

Transitions monitored, optimized parameters and retention time for LC-MS/MS analysis.

Substrate	Transition	CT	VT	SG	AG	ISG	CE	RT (min)
Amprenavir	506.3 → 245.2	270	300	60	2	30	17	2.68
Atazanavir	705.4 → 168.1	170	300	50	0	40	43	3.16
Darunavir	548.3 → 392.3	275	300	30	5	20	12	2.7
Lopinavir	629.4 → 155.2	170	300	50	0	40	38	3.4
Indinavir	614.5 → 421.3	275	300	50	5	10	32	2.94
Nelfinavir	568.3 → 330.1	275	300	50	10	10	30	3.3
Ritonavir	721.3 →140.0	220	300	60	10	25	57	3.19
	721.3 →197.0						35	
	721.3 →268.1						24	
	721.3 →296.0						16	
Saquinavir	671.5 → 570.4	275	300	60	55	10	29	3.25
Tipranavir	603.3 → 411.1	280	300	60	0	10	21	3.34
	603.3 → 585.4						14	

CT, capillary temperature; VT, vaporizing temperature; SG, sheet gas; AG, auxiliary gas; ISG, ion sweep gas; CE, collision energy; RT, retention time. All parameters (except for retention time) are expressed in arbitrary units.

Table 1

Uptake clearance values of HIV PI determined in suspended rat hepatocytes. The relative uptake, calculated as the percentage of the active/passive uptake to the total uptake, is shown in parentheses.

	Uptake clearance in suspended rat hepatocytes (µl/min/million cells)		
Compound	$Cl_{upt, active}$	$Cl_{upt, passive}$	$Cl_{upt, total}$
Amprenavir	180.5 ± 26.1 (69.9)	77.7 ± 4.7 (30.1)	258.2 ± 25.7
Atazanavir	194.5 ± 43.1 (91.3)	18.5 ± 6.0 (8.7)	213 ± 42.7
Darunavir	163.3 ± 15.4 (82.4)	34.8 ± 11.8 (17.6)	198.2 ± 9.8
Indinavir	83.8 ± 4.4 (92.2)	7.1 ± 3.5 (7.8)	90.9 ± 2.8
Lopinavir	599.4 ± 29.9 (89.6)	69.6 ± 17.4 (10.4)	669.0 ± 24.3
Nelfinavir	209.7 ± 36.4 (42.5)	284.2 ± 27.2 (57.5)	493.9 ± 24.2
Ritonavir	474.3 ± 38.1 (79.6)	121.2 ± 23.2 (20.4)	595.5 ± 30.2
Saquinavir	195.7 ± 19.4 (68.4)	90.6 ± 13.6 (31.6)	286.3 ± 13.9
Tipranavir	324.8 ± 26.3 (70.3)	137.2 ± 16.8 (29.7)	461.9 ± 20.3

Table 2

Michaelis-Menten parameters for metabolism of HIV PI in pooled rat liver microsomes.

Substrate	Km (nM)	Vmax (pmol/min/mg protein)	$Cl_{app\ int,\ met}$ (ml/min/mg protein)	$Cl_{int,\ met}$ (ml/min/mg protein)
Amprenavir	162 ± 60	163 ± 17	1.0	1.4
Atazanavir	478 ± 84	607 ± 28	1.4	1.8
Darunavir	157 ± 21	190 ± 9	1.2	2.5
Indinavir	77 ± 15	154 ± 15	2.0	2.5
Lopinavir	236 ± 88	3220 ± 316	13.6	24.6
Nelfinavir	N.D.	N.D.	N.D.	27.4[a]
Ritonavir	N.D.	N.D.	N.D.	16.8[a]
Saquinavir	81 ± 13	1040 ± 54	12.8	21.3
Tipranavir	114 ± 36	588 ± 57	5.2	12.7

N.D., not determined; [a] Published data.[19]

Table 3

Metabolic clearance values of HIV PI measured in pooled rat liver microsomes at one concentration corresponding to the *in vivo* blood concentration at the mean residence time.

Substrate	MRT (min)	Unbound blood conc after time window corresponding to MRT (nM)	$Cl_{int, met}$ (µl/min/mg protein)
Amprenavir	37.9 ± 8.4	2382	52
Atazanavir	105.9 ± 65.5	66.7	1200
Darunavir	41.1 ± 1.1	1465.7	120
Indinavir	31.6 ± 4.5	2166	74
Lopinavir	61.4 ± 12.2	42.3	11564
Nelfinavir	70.6 ± 2.8	72.3	4302
Ritonavir	156.2 ± 31.9	100.5	335
Saquinavir	76.6 ± 17.1	40.5	12312
Tipranavir	116.9 ± 3.8	11.5	6534

Table 4

Pharmacokinetic parameters of HIV PI after intravenous administrations in rats. HIV PI were dissolved in a mixture of ethanol, DMSO and saline (ratio 1:1:2) and intravenously administered via the lateral tail vein at 10 mg/kg (except for SQV; 5 mg/kg).

Compound	Blood clearance Cl_b (ml/min/kg)	Distribution volume Vd (ml)
Amprenavir	24.0 ± 4.8	345.2 ± 118.7
Atazanavir	36.7 ± 15.4	1166.5 ± 273.1
Darunavir	29.0 ± 6.2	452.8 ± 99.2
Indinavir	35.4 ± 8.5	418.3 ± 150.4
Lopinavir	47.0 ± 1.1	1204.4 ± 236.1
Nelfinavir	36.9 ± 11.6	945.6 ± 230.9
Ritonavir	12.0 ± 2.3	755.3 ± 97.6
Saquinavir	36.1 ± 7.4	1081.5 ± 111.6
Tipranavir	2.2 ± 0.4	106.9 ± 16.8

Table 5

Scaled intrinsic uptake and metabolic clearance value for all HIV PI. The *in vitro* intrinsic clearance values for uptake ($Cl_{upt,\ active}$ and $Cl_{upt,\ passive}$) and metabolism ($Cl_{int,met}$) were scaled to the whole liver by applying reported scaling factors.

	Scaled intrinsic clearance (ml/min/kg)			
	Uptake		Metabolism	
Compound	Active	Passive	Michaelis-Menten	at MRT[a]
Amprenavir	866 ± 125	373 ± 22	2496	95.6
Atazanavir	934 ± 207	89 ± 29	3282	2208.6
Darunavir	784 ± 74	167 ± 57	4589	220.6
Indinavir	402 ± 21	34 ± 17	4683	135.6
Lopinavir	2877 ± 143	334 ± 84	45338	21277.5
Nelfinavir	1007 ± 175	1364 ± 131	50377	7915.6
Ritonavir	2277 ± 183	582 ± 112	31003	616.5
Saquinavir	939 ± 93	435 ± 65	39242	22653.9
Tipranavir	1559 ± 126	658 ± 81	23407	12022.5

[a] refers to the scaled intrinsic clearance measured for a concentration observed at time equal to the mean residence time (MRT) in vivo.

Table 6

Experimentally determined fraction unbound in plasma and blood-plasma portioning ratio for all HIV PI. Fraction unbound in blood was calculated according to equation 8.

	Protein binding		
Compound	fu_{plasma}	Rb	fu'_{blood}
Amprenavir	0.32	0.87	0.16
Atazanavir	0.075	0.85	0.04
Darunavir	0.3	0.67	0.2
Indinavir	0.49	1.2	0.19
Lopinavir	0.021	0.62	0.02
Nelfinavir	0.035	0.85	0.02
Ritonavir	0.037	0.70	0.02
Saquinavir	0.051	0.82	0.03
Tipranavir	0.001	0.62	0.0004

Figure 4

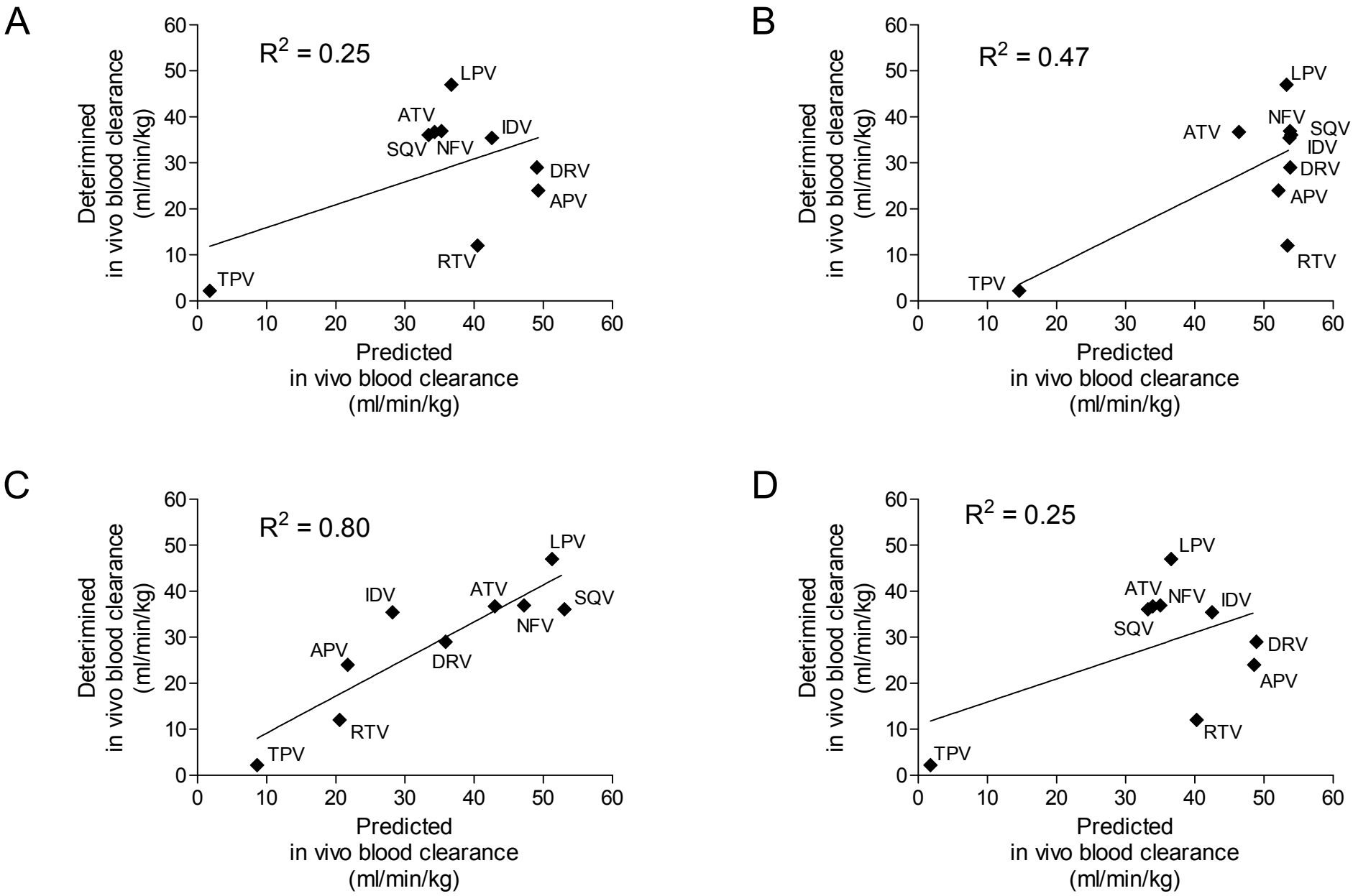
A
R^2 = 0.25
LPV
ATV
IDV
SQV
NFV
DRV
APV
RTV
TPV
Deterimined in vivo blood clearance (ml/min/kg)
Predicted in vivo blood clearance (ml/min/kg)
B
R^2 = 0.47
LPV
NFV
SQV
ATV
IDV
DRV
APV
RTV
TPV
Deterimined in vivo blood clearance (ml/min/kg)
Predicted in vivo blood clearance (ml/min/kg)
C
R^2 = 0.80
LPV
IDV
ATV
SQV
NFV
APV
DRV
RTV
TPV
Deterimined in vivo blood clearance (ml/min/kg)
Predicted in vivo blood clearance (ml/min/kg)
D
R^2 = 0.25
LPV
ATV
NFV
IDV
SQV
DRV
APV
RTV
TPV
Deterimined in vivo blood clearance (ml/min/kg)
Predicted in vivo blood clearance (ml/min/kg)

Figure 5

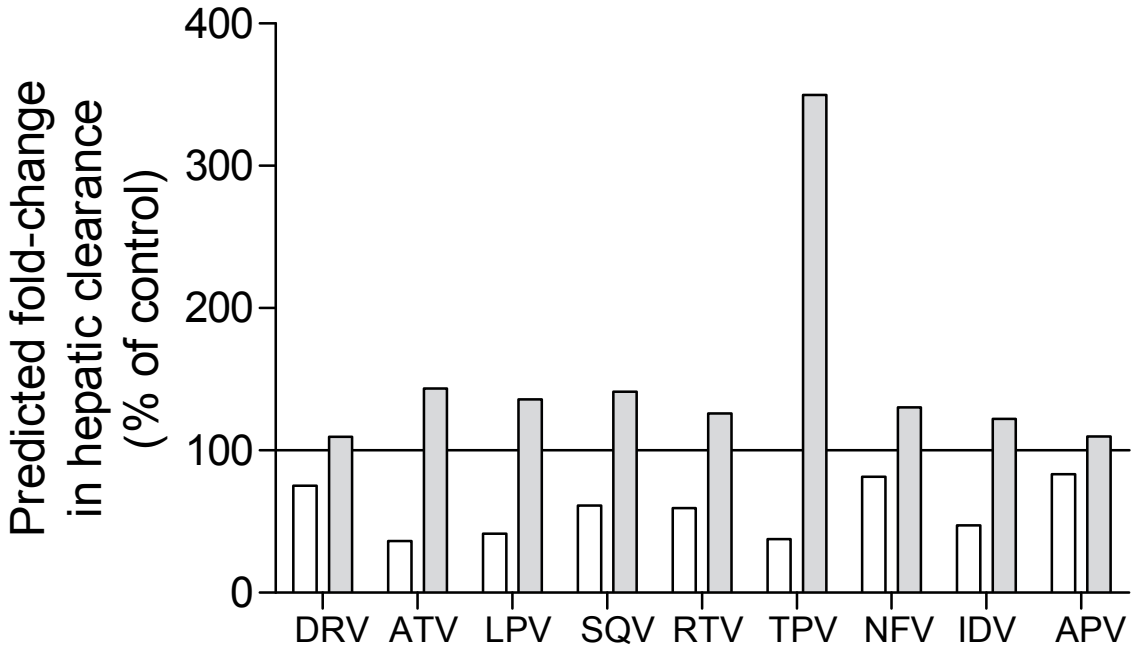
Predicted fold-change
in hepatic clearance
(% of control)
400
300
200
100
0
DRV
ATV
LPV
SQV
RTV
TPV
NFV
IDV
APV

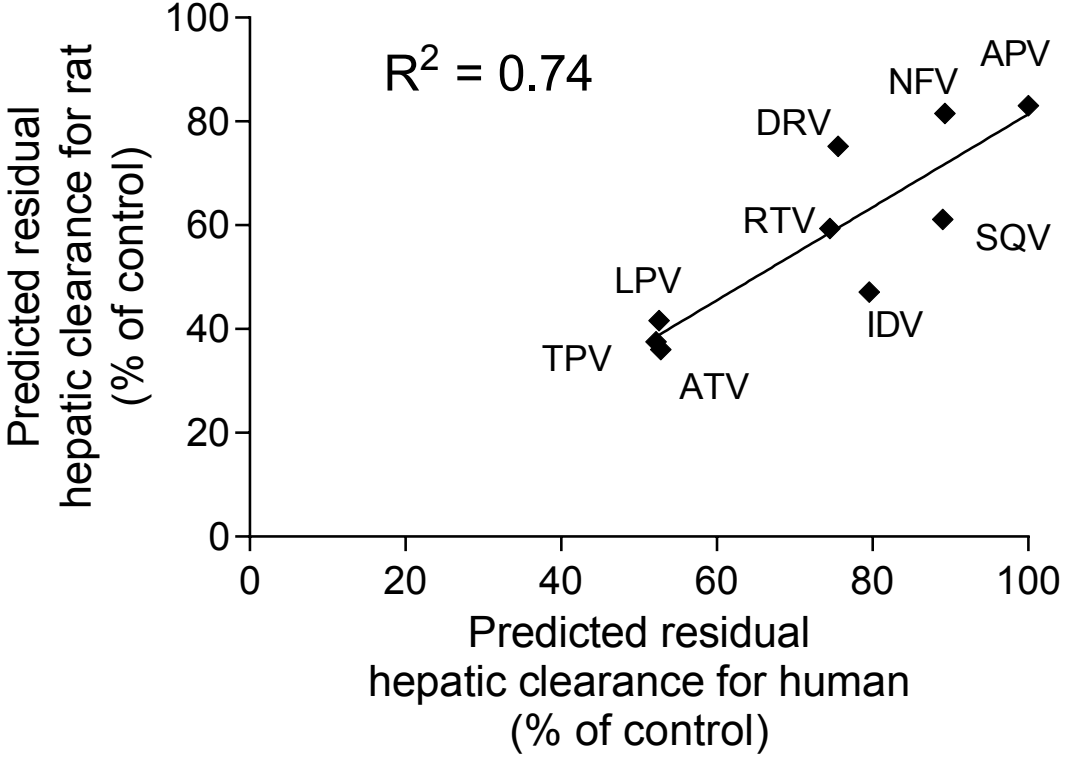
R^2 = 0.74
APV
NFV
DRV
RTV
SQV
LPV
IDV
TPV
ATV
100
80
60
40
20
0
0
20
40
60
80
100
Predicted residual hepatic clearance for rat (% of control)
Predicted residual hepatic clearance for human (% of control)

Figure 2

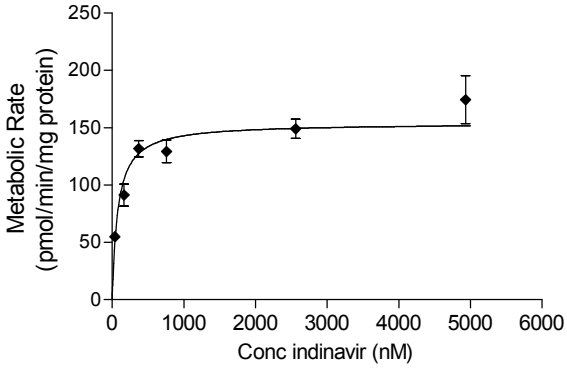
Metabolic Rate
(pmol/min/mg protein)
250
200
150
100
50
0
0
1000
2000
3000
4000
5000
6000
Conc indinavir (nM)

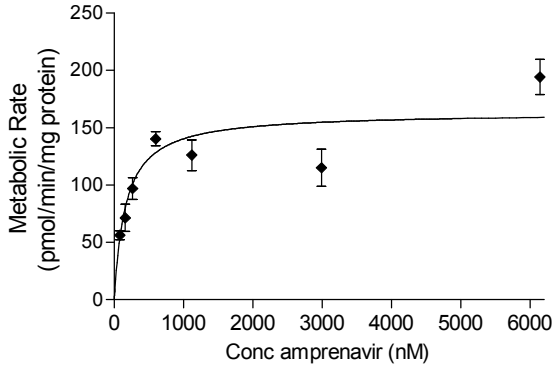
Metabolic Rate
(pmol/min/mg protein)
250
200
150
100
50
0
0
1000
2000
3000
4000
5000
6000
Conc amprenavir (nM)

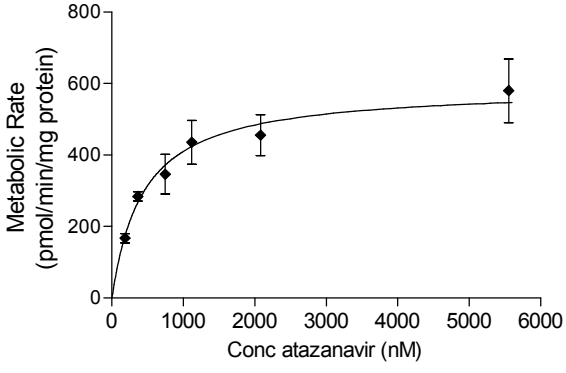
Metabolic Rate
(pmol/min/mg protein)
800
600
400
200
0
0
1000
2000
3000
4000
5000
6000
Conc atazanavir (nM)

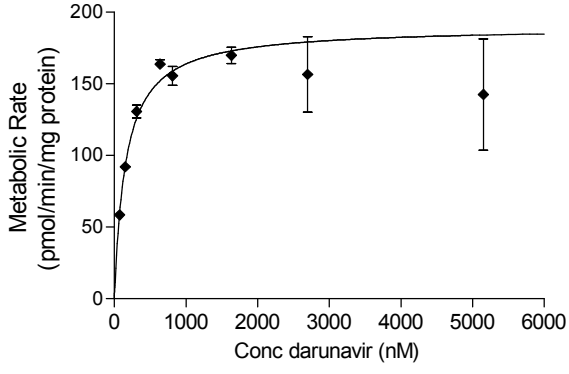
Metabolic Rate
(pmol/min/mg protein)
200
150
100
50
0
0
1000
2000
3000
4000
5000
6000
Conc darunavir (nM)

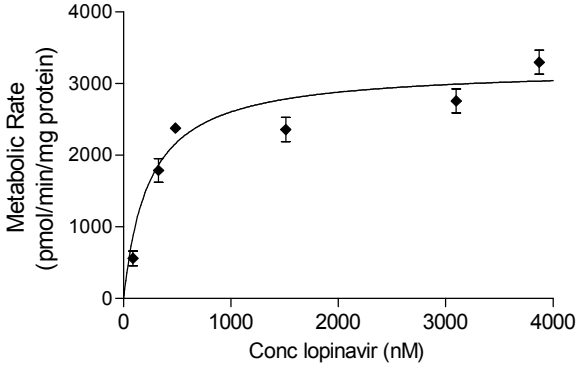
Metabolic Rate
(pmol/min/mg protein)
4000
3000
2000
1000
0
0
1000
2000
3000
4000
Conc lopinavir (nM)

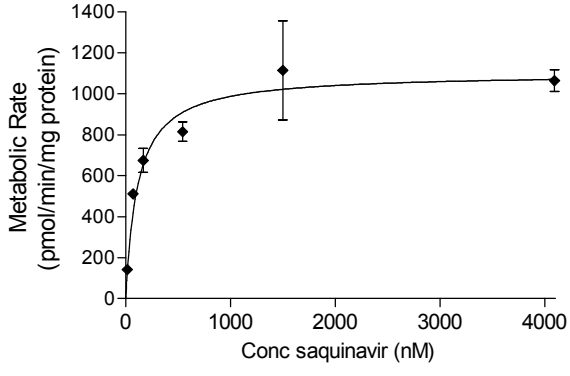
Metabolic Rate
(pmol/min/mg protein)
1400
1200
1000
800
600
400
200
0
0
1000
2000
3000
4000
Conc saquinavir (nM)

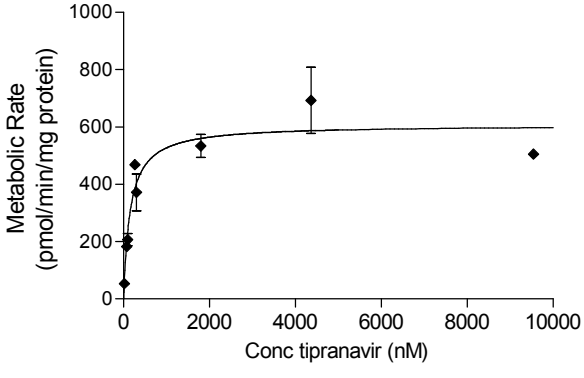
Metabolic Rate
(pmol/min/mg protein)
1000
800
600
400
200
0
0
2000
4000
6000
8000
10000
Conc tipranavir (nM)

Figure 3

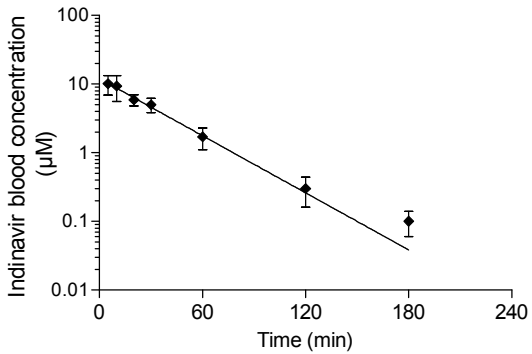
Indinavir blood concentration (μM)
100
10
1
0.1
0.01
0
60
120
180
240
Time (min)

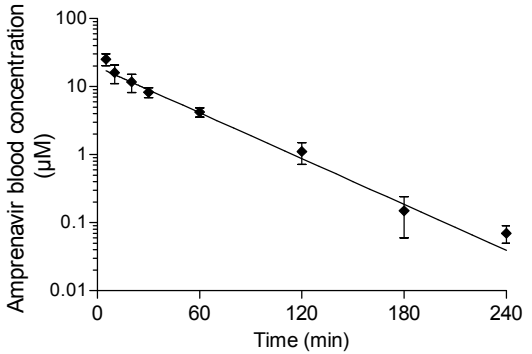
Amprenavir blood concentration (μM)
100
10
1
0.1
0.01
0
60
120
180
240
Time (min)

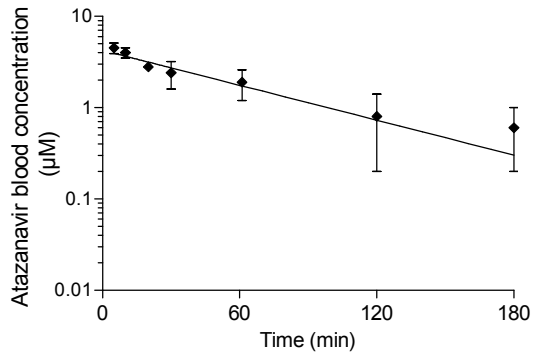
Atazanavir blood concentration (μM)
10
1
0.1
0.01
0
60
120
180
Time (min)

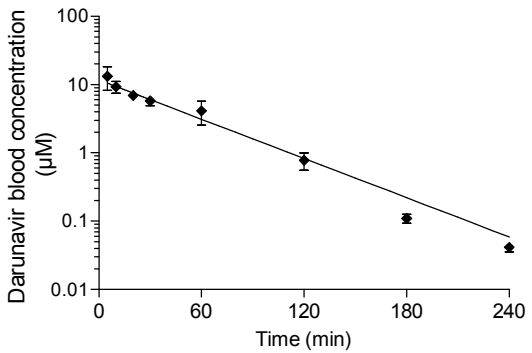
Darunavir blood concentration (μM)
100
10
1
0.1
0.01
0
60
120
180
240
Time (min)

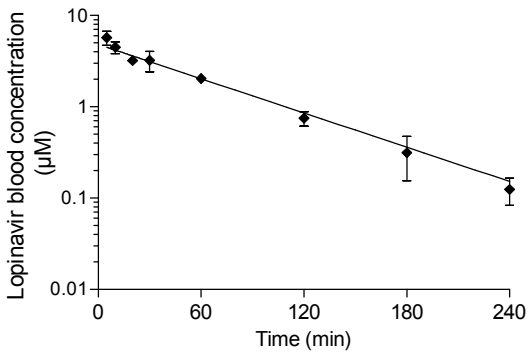
Lopinavir blood concentration (μM)
10
1
0.1
0.01
0
60
120
180
240
Time (min)

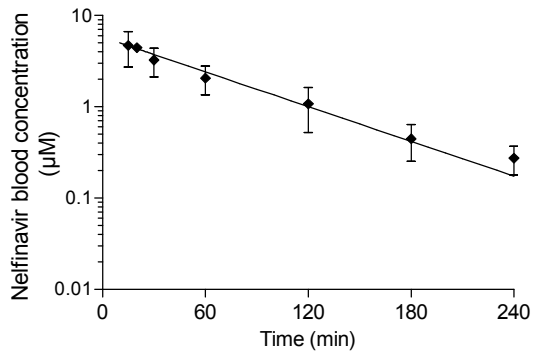
Nelfinavir blood concentration (μM)
10
1
0.1
0.01
0
60
120
180
240
Time (min)

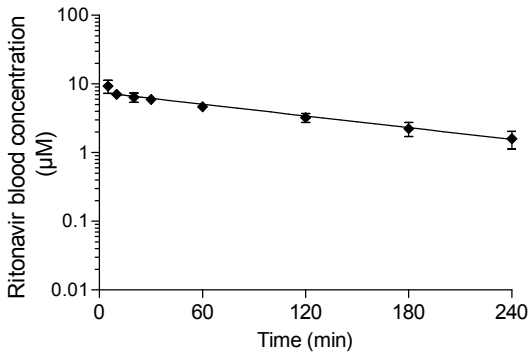
Ritonavir blood concentration (μM)
100
10
1
0.1
0.01
0
60
120
180
240
Time (min)

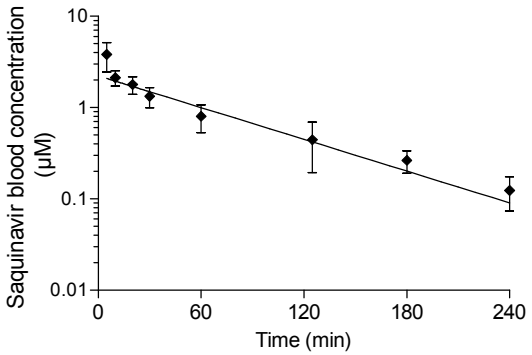
Saquinavir blood concentration (μM)
10
1
0.1
0.01
0
60
120
180
240
Time (min)

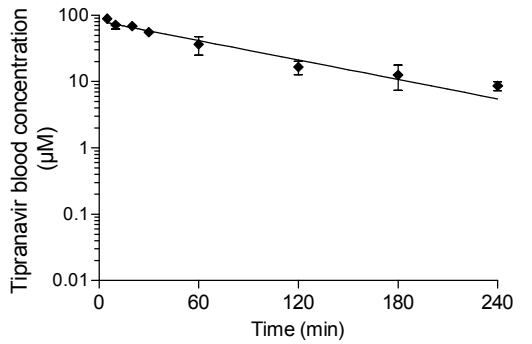
Tipranavir blood concentration (μM)
100
10
1
0.1
0.01
0
60
120
180
240
Time (min)